ISSN(Online) : 2319-8753
ISSN (Print) : 2347-6710

International Journal of Innovative Research in Science, Engineering and Technology

(An ISO 3297: 2007 Certified Organization)

Website: www.ijirset.com

Vol. 6, Issue 6, June 2017

Effect of Zinc Concentration on ZnO Nanostructured Films Synthesized by SILAR Technique

Hiten Sarma[1*], Dhruba Chakrabortty[2], Kanak Ch Sarma[3]

* Associate Professor, Department of Physics, B.N.College, Dhubri, India[1]

Principal, B.N.College, Dhubri, India[2]

Professor, Department of Instrumentation & USIC, Gauhati University, Guwahati, India[3]

ABSTRACT: Nanostructured zinc oxide thin films have been synthesized onto suitably cleaned glass substrates by SILAR (Successive Ionic Layer Adsorption and Reaction) method. X-ray diffraction study confirms the formation of nanocrystalline hexagonal wurtzite phase of zinc oxide in the films. Lattice constant is determined using Nelson Riley plots. Using X-ray broadening, crystallite sizes and lattice strain have been studied by using Williamson – Hall (W-H) method and size-strain plot method. The physical parameters such as strain, stress and energy density were calculated using modified W-H method. Morphology of the prepared films and the elemental composition were detected by using Scanning Electron Microscope (SEM) with Energy Dispersive X-Ray Analysis (EDX) and ultra-high resolution transmission electron microscope (UHRTEM).Optical properties have been studied by UV-Vis study and photoluminescence intensity.

KEYWORDS: XRD, Williamson–Hall plot, Nelson-Riley plot, Size–strain plot, UHRTEM, SEM, Band gap

I. INTRODUCTION

Nanostructured materials have drawn attentions to the researchers due to the unique physical and chemical properties of nonmaterial, which are different from those of either the bulk materials or single atoms [1]. The reduction of the size of materials causes a deviation of their physical and chemical properties from the bulk; and such resultant materials (nanocrystals) are known to possess potential applications and novel properties [2].Among the different metal oxide films, ZnO have attracted much interest as it is one of the most important II- VI wide band gap (WBG) semiconducting material with a band gap of around 3.2-3.37 eV at room temperature [3,4] with a number of interesting physical properties. Some of the favorable aspects of ZnO include its radiation hardness, biocompatibility, its high transparency in visible region and high electron mobility. ZnO has been extensively used as a window material for solar cells due to the high transmittance in the visible region and its low electrical resistivity [4]. Among different physical forms, the thin films of ZnO find a multitude of immensely important applications in electronic and optoelectronic devices such as transparent conductors, gas sensor, surface acoustic wave devices, heat mirrors etc [5]. ZnO is attractive for optoelectronic applications such as photo detectors, light emitting diodes and electro and photoluminescence devices[6] due to the direct band gap and the large exciton binding energy of 60 meV [7-9]. It has potential applications in ultra violet light emitting devices, laser devices and daylight blind UV detectors [4]. ZnO has two stable crystalline structures, hexagonal wurtzite and cubic zinc blende. The wurtzite structure is the most stable phase at ambient conditions. ZnO thin films have been obtained by pulsed laser deposition [6,7,10,11], RF magnetron sputtering [12], spray pyrolysis [13,14] and sol–gel [15],chemical vapor deposition (CVD)[16-18], photo atomic layer deposition[19], metal oxide chemical vapor deposition(MOCVD)[20], electro deposition[21], Chemical bath deposition (CBD)[22,23]

ISSN(Online) : 2319-8753
ISSN (Print) : 2347-6710

International Journal of Innovative Research in Science, Engineering and Technology

(An ISO 3297: 2007 Certified Organization)

Website: www.ijirset.com

Vol. 6, Issue 6, June 2017

and successive ionic layer adsorption and reaction (SILAR)[24] etc. We have also used SILAR (Successive Ionic Layer Adsorption and Reaction) technique for the preparation of thin films which is presently attracting considerable attention, as it does not require sophisticated instrumentation like vacuum system and other expensive equipment. Simple equipment like hot plate with magnetic stirrer is needed for this method [25].

Nelson Riley plot has been used by many research groups for calculating the lattice constant of a cubic system [26]. We have also used it for the same purpose. Crystallite size and lattice strain and stress have been calculated using Williamson Hall method [27] and Size-Strain plot (SSP) have also been used for finding size and strain of the prepared nanocrystals [28, 29], which are also used here.

X-ray diffraction (XRD) patterns of ZnO samples were recorded in PANalytical X'Pert Pro XRD with CuKα radiation (k = 1.54056 A°) at room temperature. Surface morphology was analysed by ultra high resolution transmission electron microscope (UHRTEM) (JEM 2100) operated at 200 kV. Study of SEM analysis was done by Zeiss Sigma-VP model and EDX analysis was done by Oxford X-max model. The optical absorbance spectra were recorded by UV-Vis spectrophotometer (UV-1800, SHIMADZU) and photoluminescence spectra were recorded by using F-2500 Fluorescence spectrophotometer.

II. EXPERIMENTAL

2.1 Cleaning of the substrate

The microscope glass substrate was cleaned with following steps (1) washed with mild detergent, (2) rinsed with distilled water, (3) dipped in dilute chromic acid for three hours (4) rinsed thoroughly with distilled water and (5) heated at 20^0C for 10 minutes by keeping the substrate vertically.

2.2 Deposition of thin film

Based on SILAR method the cleaned glass substrate was immersed alternatively in the zinc complex (at room temperature) for a known standardized time followed by immersion in hot water (near boiling point) for the same time for hydrogenation. The sodium zincate (zinc complex) bath was prepared by addition of a solution sodium hydroxide (NaOH pellets, Merck, mol. wt. 40) to an aqueous solution of zinc nitrate $Zn(NO_3)_2.6H_2O$ until pH of the complex becomes 12. Initially a white precipitate of zinc hydroxide appeared according to the reaction

$$Zn(NO_3)_2+2NaOH = Zn(OH)_2+2NaNO_3 \quad (1)$$

However, on further addition of NaOH the precipitate dissolved forming the Na_2ZnO_2 following the reaction

$$Zn(OH)_2 + 2NaOH = Na_2ZnO_2 + 2H_2O \quad (2)$$

Thus the overall reaction leading to the formation of sodium zincate is obtained by adding equations (1) and (2)

$$Zn(NO_3)_2 + 4NaOH = Na_2ZnO_2 + 2NaNO_3 + 2H_2O \quad (3)$$

In case of sodium zincate bath, the reaction occurring on the substrate surface leading to the formation of *ZnO* may be represented as

$$Na_2ZnO_2 + H_2O = ZnO + 2NaOH \quad (4)$$

. The period of dipping the substrate in the zinc bath (30 sec) was referred as ''adsorption'' and that in H_2O (30 sec) as ''reaction''. This process forms one cycle and was repeated 50 times in order to increase the film thickness. After each cycle, the glass slide was rinsed with distilled water and after a complete cycle the films were dried with an air dryer. Finally the film was heated at 100^oC for 1 hr and allowed to cool to room temperature The precursor solutions were prepared by adding $Zn(NO_3)_2$ solutions of 0.25, 0.50, 0.75 and 1.00 molar concentrations separately to an aqueous solution of 2 M NaOH under a high stirring rate (200 rpm) condition. During the stirring process a constant temperature 30 ^{o}C was maintained for 3 h.

ISSN(Online) : 2319-8753
ISSN (Print) : 2347-6710

International Journal of Innovative Research in Science, Engineering and Technology

(An ISO 3297: 2007 Certified Organization)

Website: www.ijirset.com

Vol. 6, Issue 6, June 2017

III. RESULTS AND DISCUSSION

3.1 X-Ray Diffraction Structural Analysis

X-Ray Diffraction (XRD) pattern of the four prepared films is shown in Fig.1. According to this figure, the films are polycrystalline and the diffraction peaks of ZnO exhibited hexagonal plane (crystals have hexagonal structure) with preferred orientation of the grains along (100), (002), (101), (102), (110), (103) and (200). All evident peaks could be indexed as the ZnO wurtzite structure (JCPDS Data Card No: 36-1451). The prominent and sharp peaks suggest that the deposited films are well crystallized. It is observed that the peak position of (100) plane of 0.25 M sample, shown in Fig.1(a), shifts slightly by an amount 0.03 towards lower diffraction angle (2θ) from its corresponding value for bulk (2θ=31.76°; JCPDS 361451), indicating tensile stress. The tensile stress is enhanced in 0.5 and 0.75 M films as peak positions get shifted more towards lower diffraction angles (2θ), which are evident from Fig.1 (b) and 1(c). The shifting of diffraction angles towards left is smaller for 1.00 M films as seen from Fig.1 (d) than that for 0.75M film. Diffraction pattern corresponding to impurities is found to be absent. This proves that pure ZnO nanoparticles were as synthesized. The sharp and strong diffraction peaks confirmed the high crystalline quality of the prepared samples. The lattice parameters have been calculated using the relation

$$\frac{1}{d^2} = \frac{3}{4}\left(\frac{h^2 + hk + k^2}{a^2}\right) + \left(\frac{l^2}{c^2}\right) \qquad (5)$$

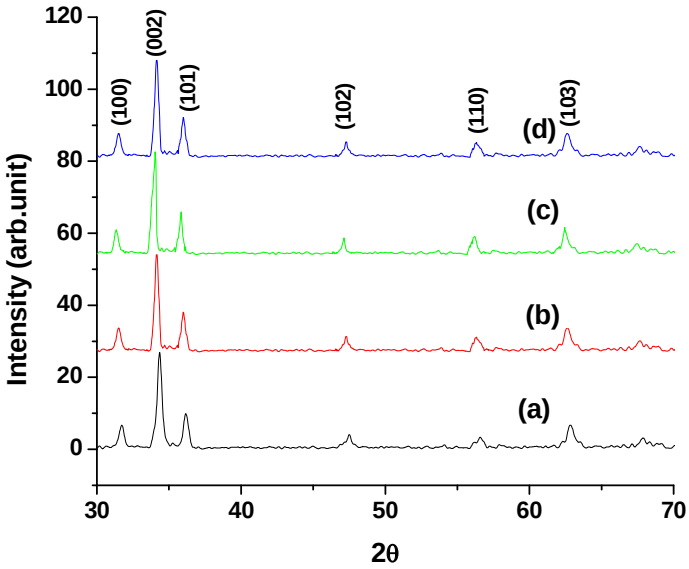

Fig. 1 XRD Patterns of ZnO films with molarities (a) 0.25 M, (b) 0.50 M and (c) 0.75M and (d) 1.00 M

ISSN(Online) : 2319-8753
ISSN (Print) : 2347-6710

International Journal of Innovative Research in Science, Engineering and Technology

(An ISO 3297: 2007 Certified Organization)

Website: www.ijirset.com

Vol. 6, Issue 6, June 2017

3.1.1 Lattice constant

Lattice parameters '*a*' and '*c*' of the hexagonal phase for ZnO were calculated according to the next expressions [30]

$$a = \frac{\lambda}{2\sin\theta}\sqrt{\frac{4}{3}(h^2+hk+k^2)+\left(\frac{a}{c}\right)^2 l^2} \quad (6)$$

$$c = \frac{\lambda}{2\sin\theta}\sqrt{\frac{4}{3}\left(\frac{c}{a}\right)^2\left(h^2+hk+k^2\right)+l^2} \quad (7)$$

The corrected values of lattice constants are estimated from the Nelson-Riley plots. The Nelson – Riley curve is a plot between the calculated 'a' for different planes and error function [31] given by

$$f(\theta) = \frac{1}{2}\left(\frac{\cos^2\theta}{\sin\theta}+\frac{\cos^2\theta}{\theta}\right) \quad (8)$$

and extrapolation to $\theta=90^0$. A typical Nelson – Riley plot for synthesized samples are shown in Fig.2 and Fig.3 and values are shown in Table1. The lattice constant 'a(corrected)' and 'c(corrected) of the film calculated using Nelson-Riley plot (Table 1) is different from its bulk value a_o = 3.253 Å and c_o = 5.215 Å . This means the particles are under strain which contributes towards broadening of the diffraction peak.

3.1.2 Film thickness measurement

If W_1 and W_2 are the weights of the substrate before and after film deposition in gm., A is the area of film deposition in cm^2 and ρ is the theoretical density of ZnO (5.6 gm/cm^3), then the film thickness is evaluated as:

$$t = \frac{w_2 - w_1}{A\rho}\times 10^7\, nm \quad (9)$$

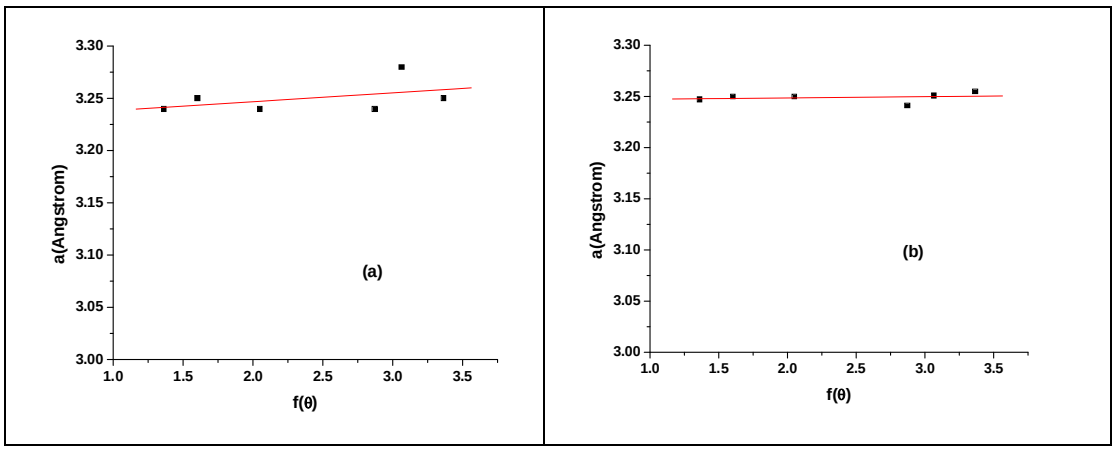

ISSN(Online) : 2319-8753
ISSN (Print) : 2347-6710

International Journal of Innovative Research in Science, Engineering and Technology

(An ISO 3297: 2007 Certified Organization)

Website: www.ijirset.com

Vol. 6, Issue 6, June 2017

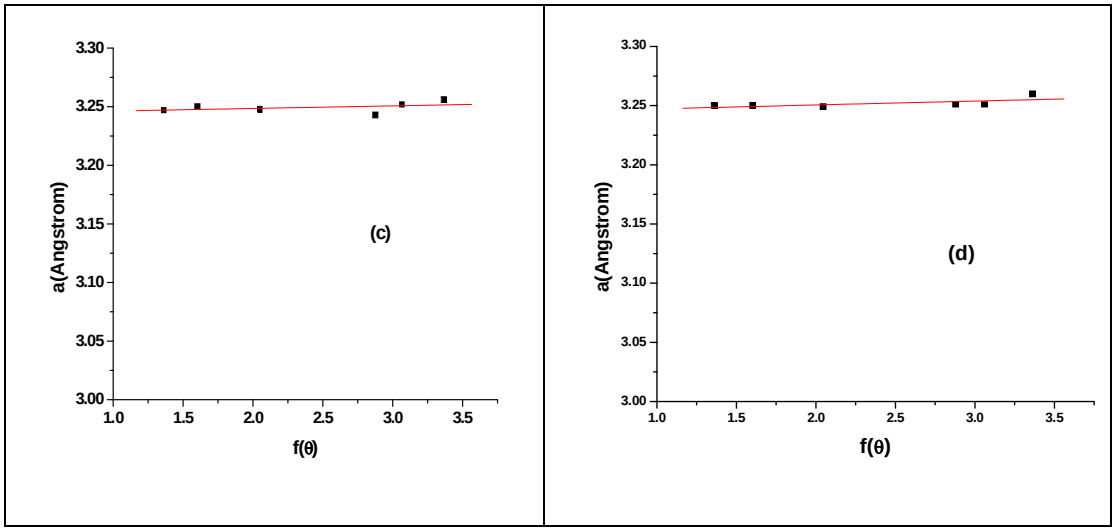

Fig. 2 Nelson–Riley plots of ZnO films for (a) 0.25 M, (b) 0.50 M, (c) 0.75 and (d) 1.00M for parameter 'a'

3.1.3 Texture Coefficient

Quantitative information concerning the preferential crystal orientation can be obtained from the texture coefficient, [32]

$$T_c(hkl) = \frac{I(hkl)/I_0(hkl)}{\frac{1}{n}\sum_n I(hkl)/I_0(hkl)} \quad (10)$$

where $T_C(hkl)$ is the texture coefficient, n is the number of diffraction peaks considered, $I(hkl)$is the measured x-ray intensity and $I_o(hkl)$ is the corresponding recorded intensity according to JCPDS card [32] Since six diffraction peaks were used, the maximum value T_C (hkl) possible is 6. The texture coefficient for the (002) orientation has been found to be 2.756 ,2.663 ,2.579 and 2.645 respectively for 0.25 M,0.50M , 0.75M and 1.00M films respectively.

3.1.4 Dislocation density

The dislocation density is a measure of the number of dislocations in a unit volume of a crystalline material. The dislocation density (δ), defined as the length of dislocation lines per unit volume are

estimated using the equation $\delta = \frac{1}{D^2}$ and they are calculated for four different samples of ZnO films prepared and are found to be 18.01×10^{14},14.89×10^{14},13.9×10^{14} and 15.26×10^{14} lines/m^2 respectively for 0.25,0.50,0.75 and 1.00 molarity films. The molarity versus dislocation density are shown in Fig.5 (d).

3.1.5 Unit cell volume

The unit cell volume for hexagonal structure can be calculated by the relation

$$V = a^2 c \sin 60 = \frac{\sqrt{3}}{2} a^2 c \quad (11)$$

The values are tabulated in table1.

3.*1.6 Crystallite size*

The crystallite size 'D' of the prepared ZnO-Films is estimated from the Scherrer's formula [33]

ISSN(Online) : 2319-8753
ISSN (Print) : 2347-6710

International Journal of Innovative Research in Science, Engineering and Technology

(An ISO 3297: 2007 Certified Organization)

Website: www.ijirset.com

Vol. 6, Issue 6, June 2017

$$\beta_D = \frac{\kappa\lambda}{D\cos\theta} \quad (12)$$

where the constant K is taken as 0.94, λ is the wavelength of the wavelength of X-rays used (λ = 1.5406 Å). β_D is the full width at half maximum of the diffraction peaks after necessary correction for instrumental broadening. The average values of Crystallite size are shown in Table2.

3.1.7 Williamson Hall method

In X-Ray Diffraction, the broadening of XRD line profile is not only due to crystallite size but also due to the presence of non-uniform strain in the material. If the size and strain broadening is present simultaneously then crystallite size and strain may be found from W–H plot. Crystal imperfections and distortion of strain induced peak broadening are related by

$$\varepsilon = \frac{\beta_S}{4\tan\theta} \Rightarrow \beta_S = 4\varepsilon\tan\theta \quad (13)$$

Depending on different 'θ' positions, the separation of size and strain broadening analysis is done using Williamson and Hall. According to Williamson and Hall

$$\beta = \beta_S + \beta_D \quad (14)$$

Substituting eq. (11) and (12) in the above equation we get,

$$\beta = \frac{\kappa\lambda}{D\cos\theta} + 4\varepsilon\tan\theta$$

$$\Rightarrow \quad \beta\cos\theta = \frac{\kappa\lambda}{D} + 4\varepsilon\sin\theta \quad (15)$$

Table 1. Structural parameters of chemically deposited ZnO film with different molarities

Molarity & thickness of the film	*hkl*	d (Å)	2θ (deg.)	JCPDS: 36-1451 d (Å)	a (Å)	f(θ)	a (corrected) (Å)	c (Å)	c (corrected) (Å)	V $(Å)^3$	$T_c(hkl)$
0.25M & 400nm	*100* *002* *101* *102* *110* *103*	2.818 2.605 2.477 1.912 1.625 1.477	31.73 34.40 36.23 47.52 56.58 62.84	2.814 2.602 2.476 1.911 1.625 1.477	3.258 3.251 3.250 3.250 3.250 3.248	3.366 3.066 2.880 2.050 1.602 1.362	3.247	5.221 5.210 5.202 5.210 5.210 5.206	5.207	47.54	0.522 2.756 0.446 0.788 0.459 1.036

ISSN(Online) : 2319-8753
ISSN (Print) : 2347-6710

International Journal of Innovative Research in Science, Engineering and Technology

(An ISO 3297: 2007 Certified Organization)

Website: www.ijirset.com

Vol. 6, Issue 6, June 2017

0.50M & 450nm	*100* *002* *101* *102* *110* *103*	2.820 2.606 2.479 1.912 1.625 1.477	31.71 34.39 36.20 47.51 56.58 62.83	2.814 2.602 2.476 1.911 1.625 1.477	3.260 3.252 3.252 3.250 3.250 3.248	3.362 3.063 2.881 2.050 1.602 1.363	3.248	5.225 5.212 5.206 5.210 5.210 5.206	5.205	47.55	0.511 2.663 0.408 0.847 0.756 0.820
0.75M & 500nm	*100* *002* *101* *102* *110* *103*	2.826 2.615 2.480 1.916 1.627 1.480	31.70 34.38 36.18 47.49 56.56 62.83	2.814 2.602 2.476 1.911 1.625 1.477	3.267 3.263 3.254 3.257 3.254 3.254	3.359 3.060 2.868 2.045 1.599 1.358	3.251	5.218 5.230 5.208 5.221 5.216 5.217	5.215	47.73	0.484 2.579 0.476 0.798 0.623 1.039
1.00M & 550nm	*100* *002* *101* *102* *110* *103*	2.820 2.605 2.478 1.911 1.625 1.478	31.75 34.40 36.22 47.52 56.58 62.85	2.814 2.602 2.476 1.911 1.625 1.477	3.260 3.251 3.251 3.249 3.250 3.250	3.362 3.060 2.880 2.047 1.601 1.362	3.247	5.225 5.210 5.204 5.207 5.210 5.210	5.202	47.49	0.504 2.645 0.401 0.832 0.723 0.814

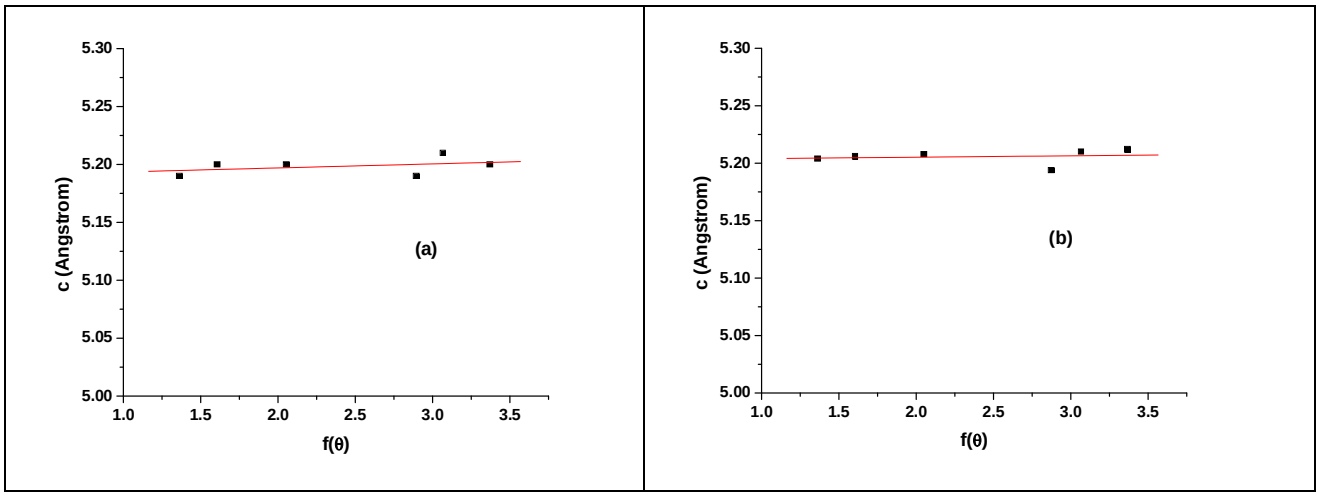

ISSN(Online) : 2319-8753
ISSN (Print) : 2347-6710

International Journal of Innovative Research in Science, Engineering and Technology

(An ISO 3297: 2007 Certified Organization)

Website: www.ijirset.com

Vol. 6, Issue 6, June 2017

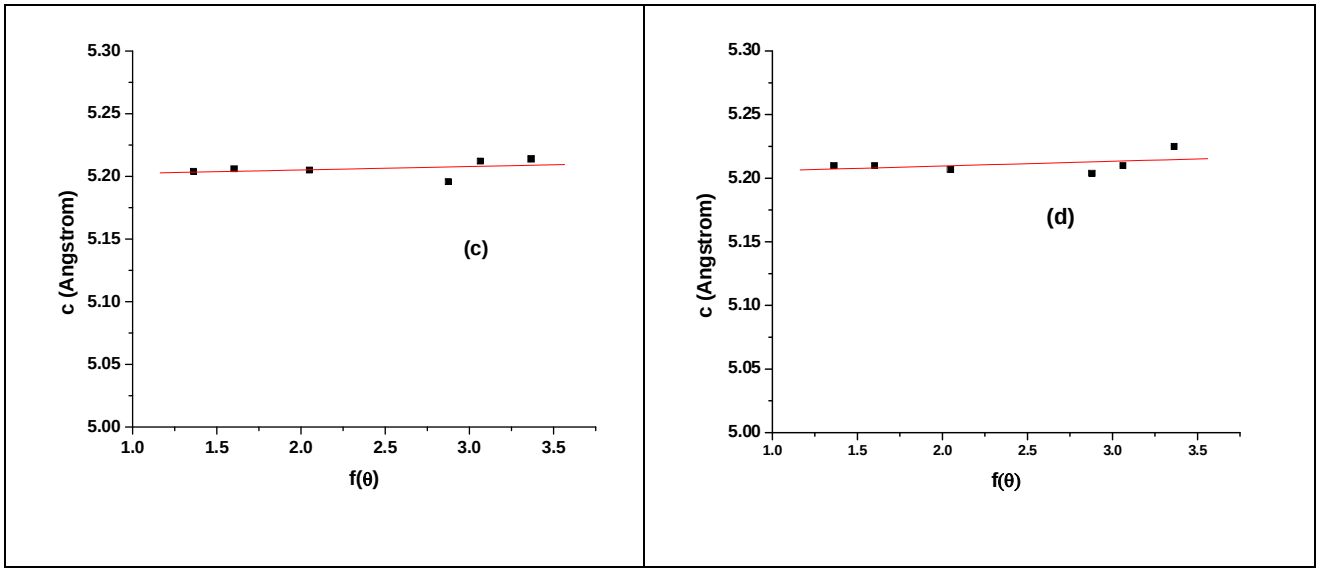

Fig. 3 Nelson–Riley plots of ZnO films for (a) 0.25 M, (b) 0.50 M (c) 0.75 M , (d) 1.00M for parameter 'c'

Equation (15) represents the uniform deformation model (UDM). Here the strain is assumed to be uniform in all crystallographic directions. A graph is drawn with 4 sinθ along X – axis and βcosθ along Y – axis (Fig.4). From the graph, strain and crystallite size are calculated from the slope and y intercept of the fitted line respectively and the values are tabulated in Table 3. It is observed that there is a gradual increase in crystallite size obtained both from Scherrer's formula and W–H plot with the increase in the molarities of the solutions till 0.75M and at 1.00 M it again decreases.(Fig. 5(a) and 5(b)). A similar kind of result has been also reported earlier by other workers [34].There is a decrease in strain with molarity (Fig.5(c)) till 0.75M and it again increases after that.

3.1.8 Size–Strain plot Method

"Size–strain plot'' (SSP) can be used for estimation of size–strain parameters for isotropic line broadening. In this method, less importance is given to the data from reflection at high angles, because, normally precision is less in those ranges of angles [35]. In this approximation method, the ''crystallite size'' profile is described by a Lorentzian function and the ''strain profile" is described by Gaussian function [36]. Then one can write

$$\left(\frac{d\beta\cos\theta}{\lambda}\right)^2 = \frac{1}{D}\left(\frac{d^2\beta\cos\theta}{\lambda}\right) + \left(\frac{\varepsilon}{2}\right)^2 \qquad (16)$$

ISSN(Online) : 2319-8753
ISSN (Print) : 2347-6710

International Journal of Innovative Research in Science, Engineering and Technology

(An ISO 3297: 2007 Certified Organization)

Website: www.ijirset.com

Vol. 6, Issue 6, June 2017

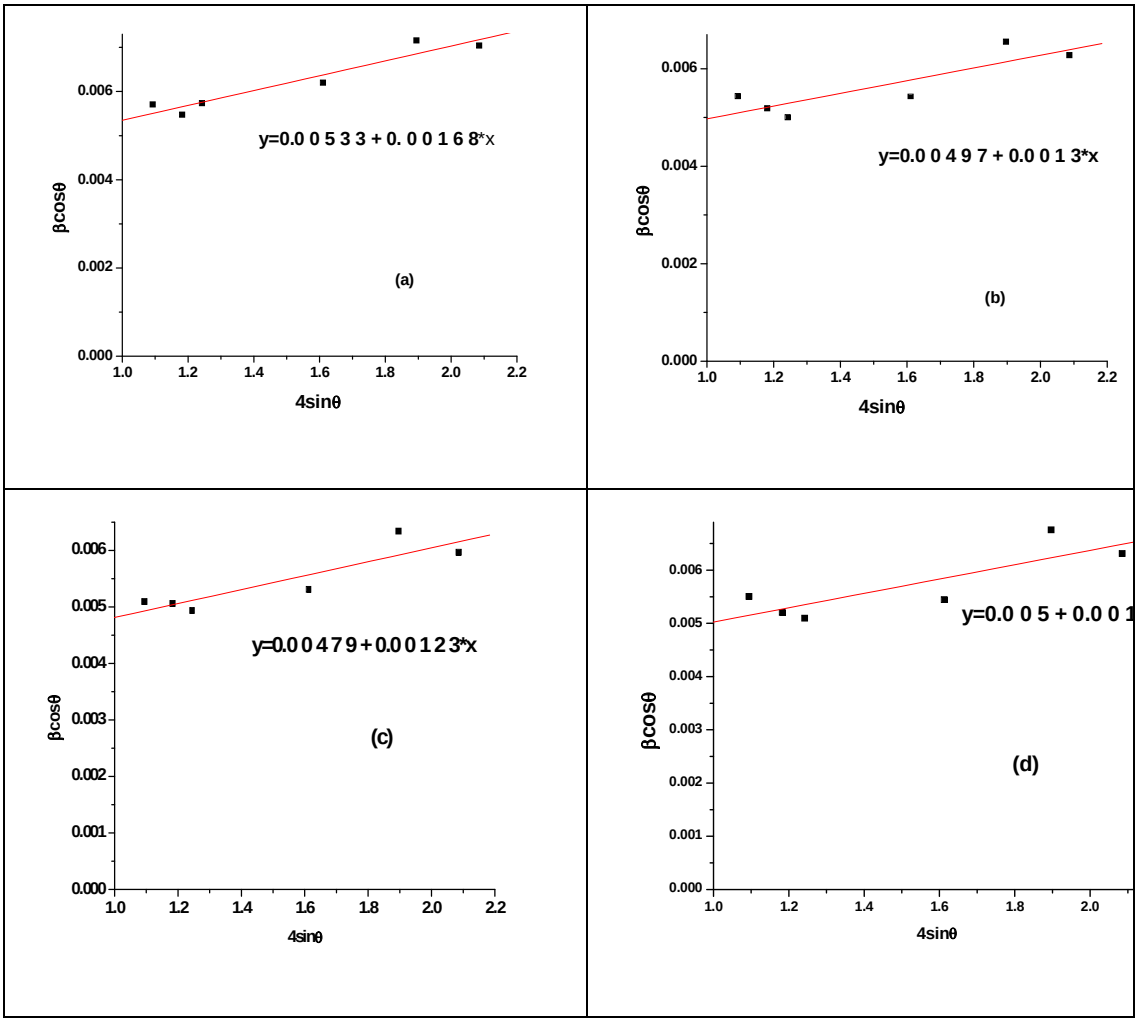

Fig. 4 W–H plots of ZnO Films for (a) 0.25 M, (b) 0.50 M and (c) 0.75M and (d) 1.00M

The term $\left(\frac{d^2\beta\cos\theta}{\lambda}\right)$ is plotted along X-axis against $\left(\frac{d\beta\cos\theta}{\lambda}\right)^2$ along Y-axis for different peak orientations of 0.25, 0.50 and 0.75M of ZnO films as shown in Fig. 6.The crystallite size is determined from the slope of the linearly fitted data and the value of strain is obtained from y-intercept. The size of the crystallite is obtained from $D = \frac{k\lambda}{slope}$ where K = 3/4 for spherical particle. The mean apparent strain is $\varepsilon_{app} = 2\left(\sqrt{y\,\text{int}\,ercept}\right)$ and the root mean square strain is obtained from $\varepsilon = \frac{\varepsilon_{app}}{2\pi\sqrt{2}}$ [37]. The estimated values of D and ε are shown in Table2.

ISSN(Online) : 2319-8753
ISSN (Print) : 2347-6710

International Journal of Innovative Research in Science, Engineering and Technology

(An ISO 3297: 2007 Certified Organization)

Website: www.ijirset.com

Vol. 6, Issue 6, June 2017

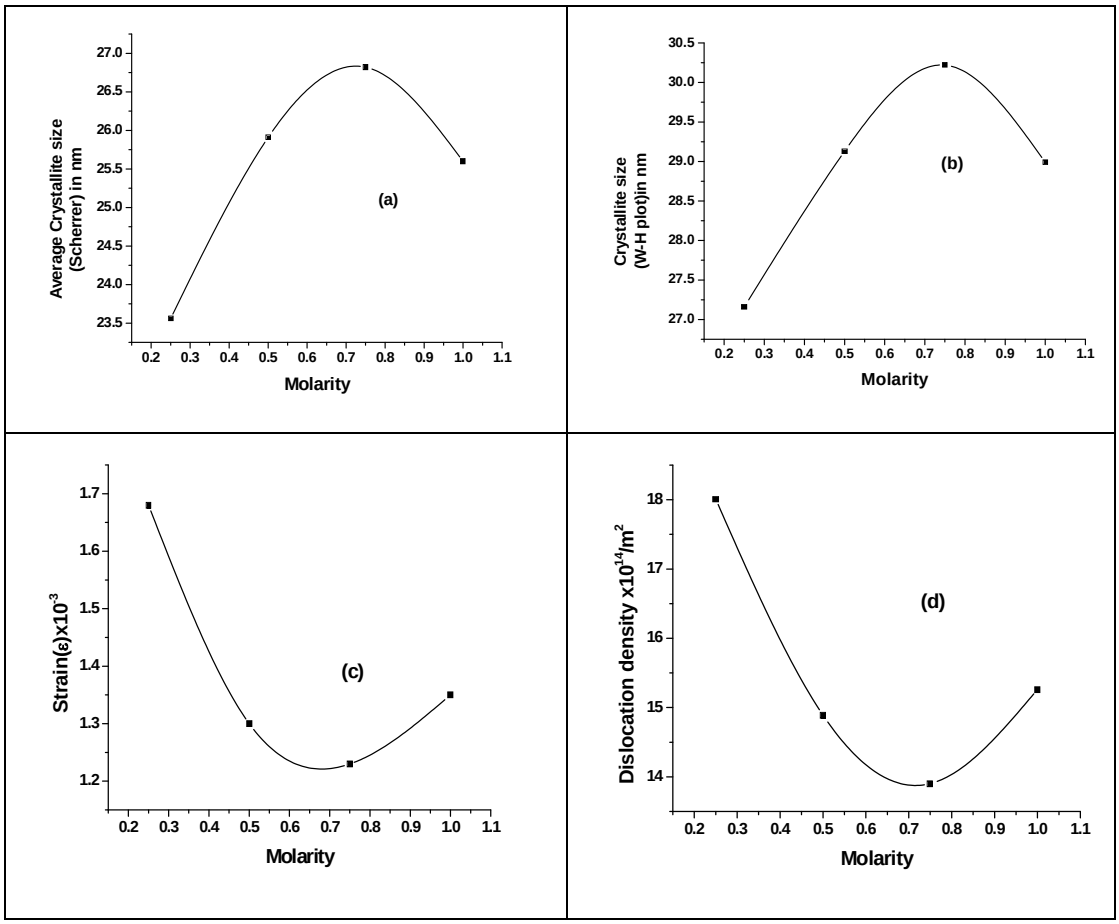

Fig.5(a)Avg. Crystallite size from Scherrer's formula versus molarity. (b) Crystallite size from W–H plot versus molarity. (c) Strain from W–H plot versus molarity (d) Dislocation density versus molarity of ZnO films

3.1.9 Modified Williamson – Hall method

From Uniform Stress Deformation Model (USDM), strain is calculated from Hooke's law maintaining linear proportionality between stress and strain given by $\sigma = Y\varepsilon$ where σ is the stress, ε is the strain and Y is the Young's modulus. Applying Hooke's law approximation to eq. (15), we get

$$\beta \operatorname{Cos}\theta = \frac{\kappa\lambda}{D} + \frac{4\sigma}{Y}\operatorname{Sin}\theta \qquad (17)$$

ISSN(Online) : 2319-8753
ISSN (Print) : 2347-6710

International Journal of Innovative Research in Science, Engineering and Technology

(An ISO 3297: 2007 Certified Organization)

Website: www.ijirset.com

Vol. 6, Issue 6, June 2017

Table2. Size and strain of nanocrystals of ZnO films prepared using Scherrer method and SSP method

Molarity of Solution	Scherrer method	SSP method	
	D (nm)	D(nm)	Strain Ɛ x 10^{-3}
0.25M	23.56	35.75	1.411
0.50M	25.91	37.38	1.274
0.75M	26.82	42.46	1.245
1.00 M	25.60	36.44	1.288

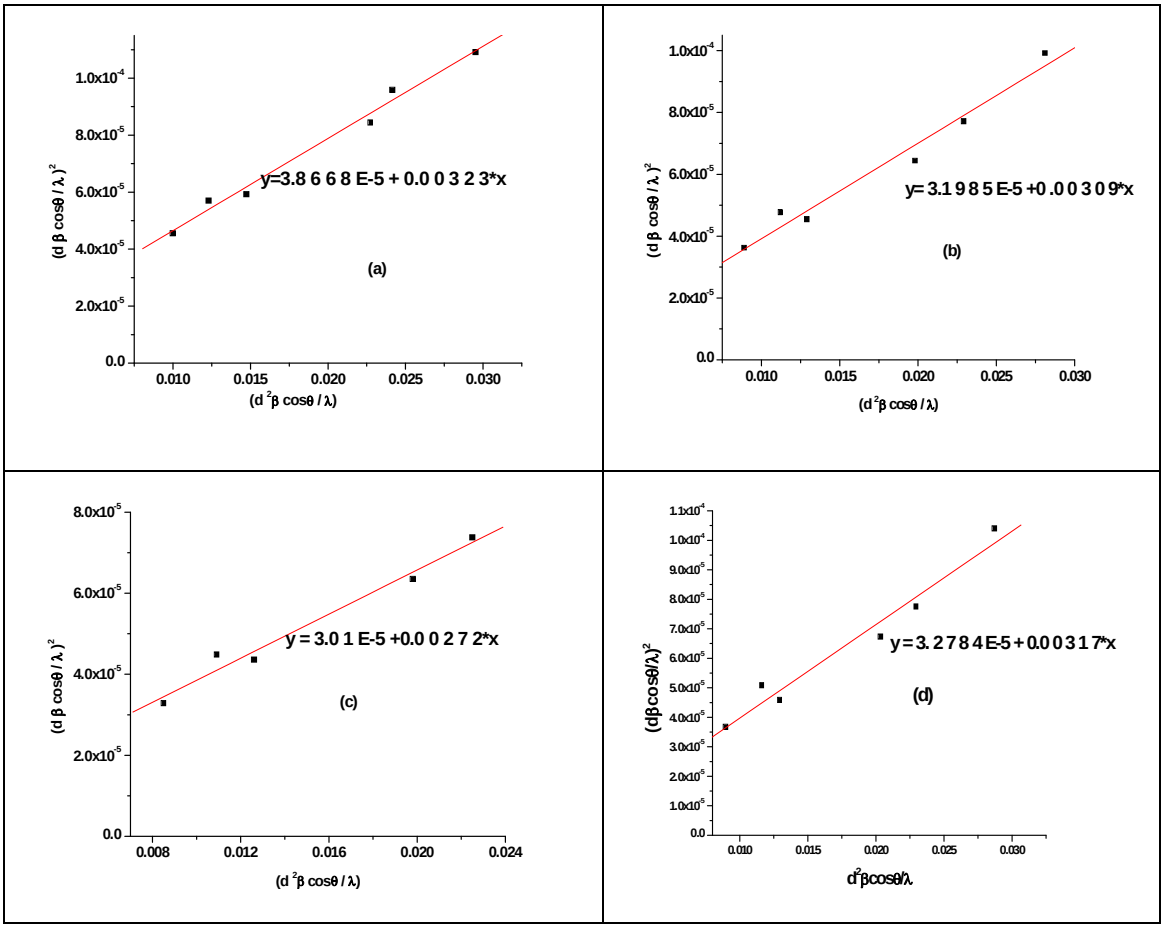

Fig.6 Size–strain plots of ZnO Films for (a) 0.25 M, (b) 0.50 M and (c) 0.75M and (d) 1.00 M

ISSN(Online) : 2319-8753
ISSN (Print) : 2347-6710

International Journal of Innovative Research in Science, Engineering and Technology

(An ISO 3297: 2007 Certified Organization)

Website: www.ijirset.com

Vol. 6, Issue 6, June 2017

Again, the modulus of elasticity or Young's modulus '*Y*' for hexagonal crystal is given by the relation [38]

$$Y_{hkl} = \frac{\left[h^2 + \frac{(h+2k)^2}{3} + \left(\frac{al}{c}\right)^2\right]^2}{S_{11}\left[h^2 + \frac{(h+2k)^2}{3}\right]^2 + S_{33}\left(al/c\right)^4 + (2S_{13} + S_{44})\left[h^2 + \frac{(h+2k)^2}{3}\right]\left(\frac{al}{c}\right)^2} \quad (18)$$

where S_{11}, S_{13}, S_{33}, S_{44} are the elastic compliances of ZnO with values of 7.858 x10^{-12}, -2.206 x10^{-12}, 6.940x10^{-12}, 23.57 x10^{-12} $m^2 N^{-1}$, respectively[39] .Average value of Young's modulus, *Y* calculated is 130 GPa.[40].

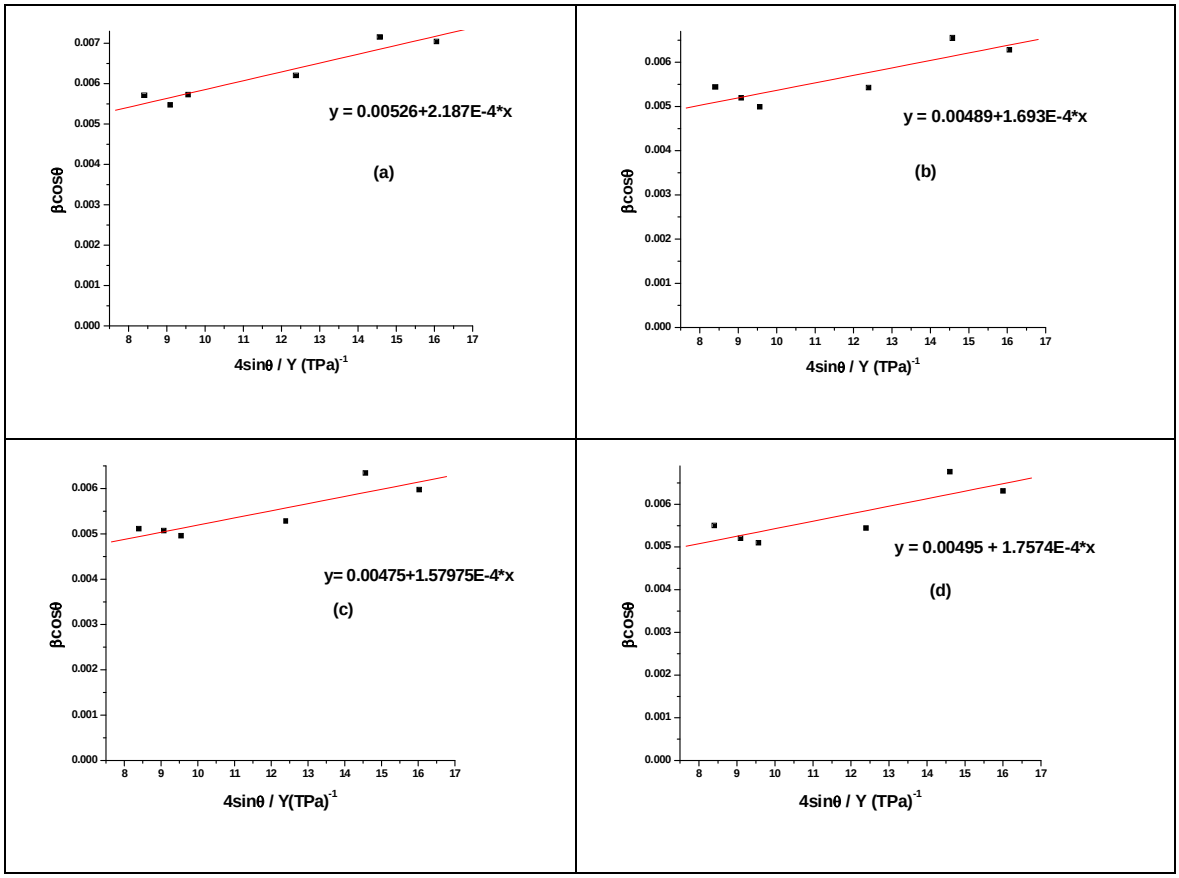

Fig. 7 Modified W–H plots of ZnO films using USDM for (a) 0.25 M, (b) 0.50 M and (c) 0.75M and (d) 1.00M

A graph is plotted between $\frac{4\sin\theta}{Y}$ along X – axis and $\beta\cos\theta$ along Y – axis (Fig.7). The stress is calculated from the slope of the graph and crystallite size from the Y intercept and the values are tabulated in Table 3. The energy density of a crystal was calculated from a model called Uniform Deformation Energy Density Model (UDEDM).

ISSN(Online) : 2319-8753
ISSN (Print) : 2347-6710

International Journal of Innovative Research in Science, Engineering and Technology

(An ISO 3297: 2007 Certified Organization)

Website: www.ijirset.com

Vol. 6, Issue 6, June 2017

According to Hooke's law, the energy density u (energy per unit volume) is $u = \frac{\varepsilon^2 Y}{2}$. Therefore, Equation (15) can be modified to the form

$$\beta \cos\theta = \frac{\kappa\lambda}{D} + 4\sin\theta\left(\frac{2u}{Y}\right)^{\frac{1}{2}} \qquad (19)$$

A graph is plotted between $4\sin\theta\left(\frac{2}{Y}\right)^{\frac{1}{2}}$ along X -axis and βcosθ along Y – axis (Fig.8).From the slope of the graph, energy density u is calculated and the crystallite size D is calculated from the Y intercept and the values are tabulated in Table 3.

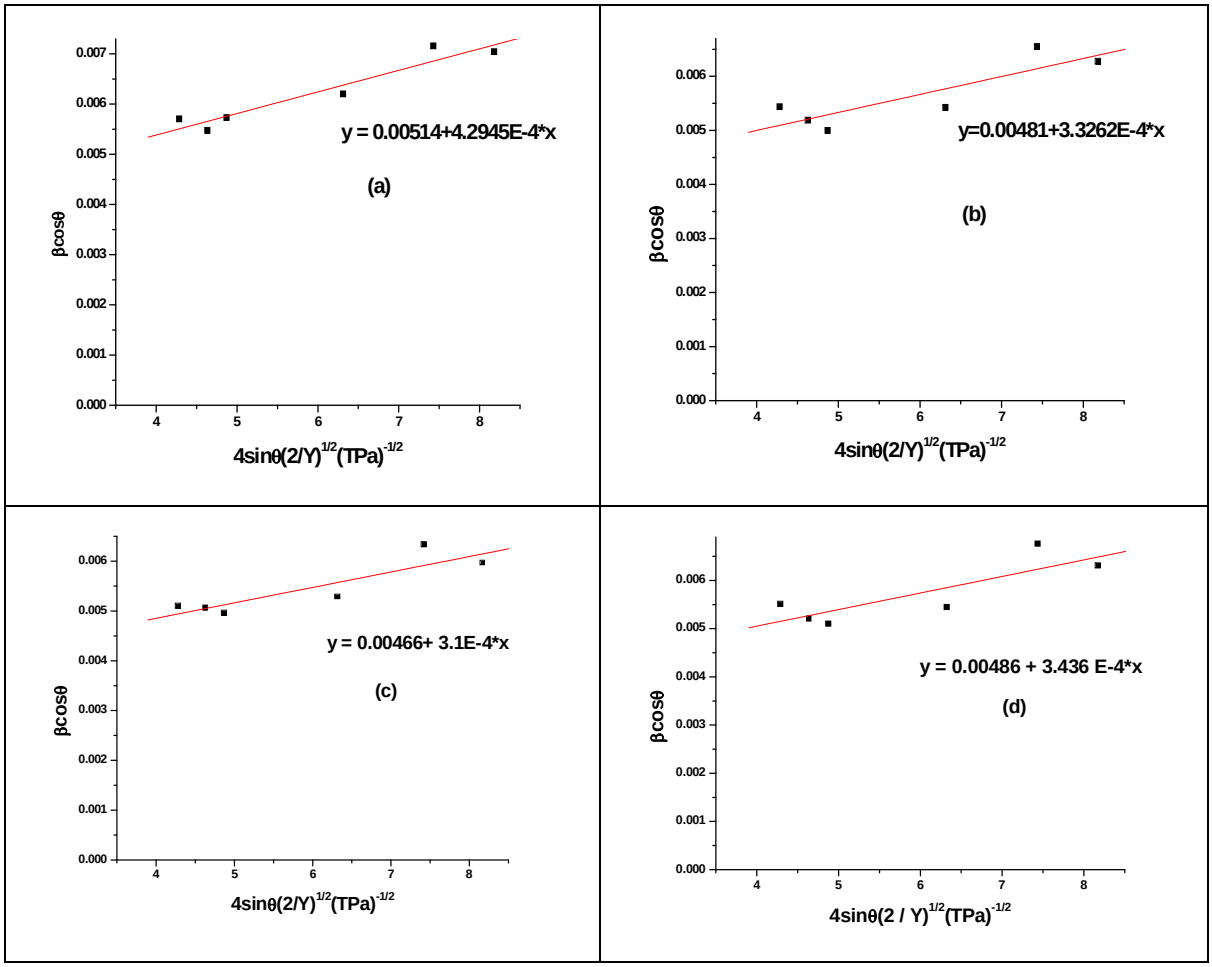

Fig. 8 Modified W–H plots of ZnO films using UDEDM for (a) 0.25 M, (b) 0.50 M and (c) 0.75M and (d) 1.00M

ISSN(Online) : 2319-8753
ISSN (Print) : 2347-6710

International Journal of Innovative Research in Science, Engineering and Technology

(An ISO 3297: 2007 Certified Organization)

Website: www.ijirset.com

Vol. 6, Issue 6, June 2017

Table3. Geometric parameters of ZnO films prepared using W-H method and modified W-H method

MOLARITY	Williamson Method								
	UDM		USDM			UDEDM			
	D (nm)	strain ϵ $x10^{-3}$	D (nm)	Strain ϵ $x10^{-3}$	stress σ (MPa)	D (nm)	strain ϵ $x10^{-3}$	Stress σ (MPa)	u (KJ/m^3)
0.25M	27.16	1.68	27.53	1.682	218.70	28.17	1.684	218.92	184.40
0.50M	29.13	1.30	29.61	1.302	169.30	30.10	1.304	169.52	110.64
0.75M	30.22	1.23	30.52	1.215	157.97	31.10	1.216	158.08	96.10
1.00M	28.99	1.35	29.25	1.352	175.74	29.83	1.348	175.20	118.06

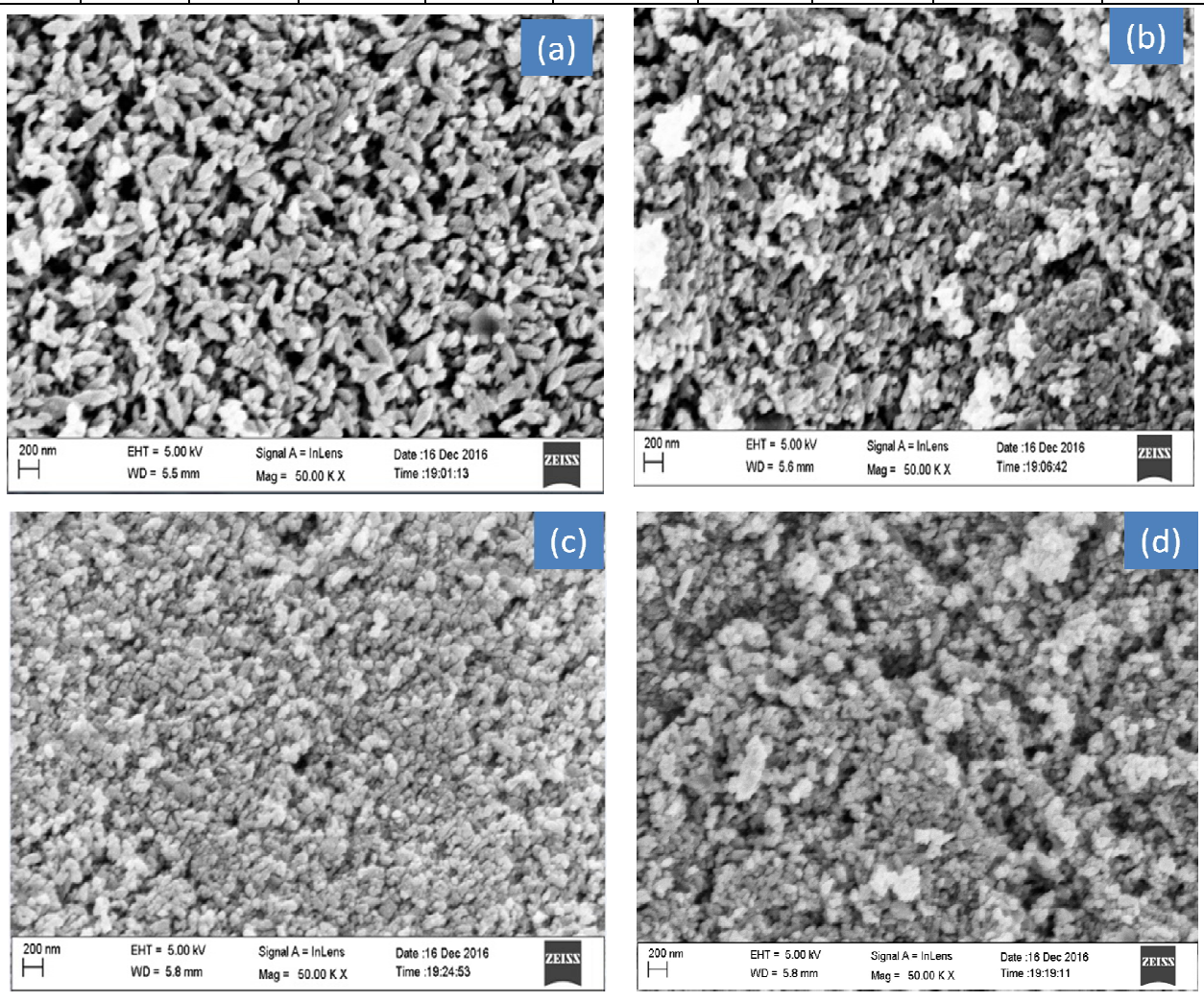

Fig.9 SEM image of ZnO thin films with molarities (a) 0.25M, (b) 0.50M ,(c) 0.75M and (d)1.00M

ISSN(Online) : 2319-8753
ISSN (Print) : 2347-6710

International Journal of Innovative Research in Science, Engineering and Technology

(An ISO 3297: 2007 Certified Organization)

Website: www.ijirset.com

Vol. 6, Issue 6, June 2017

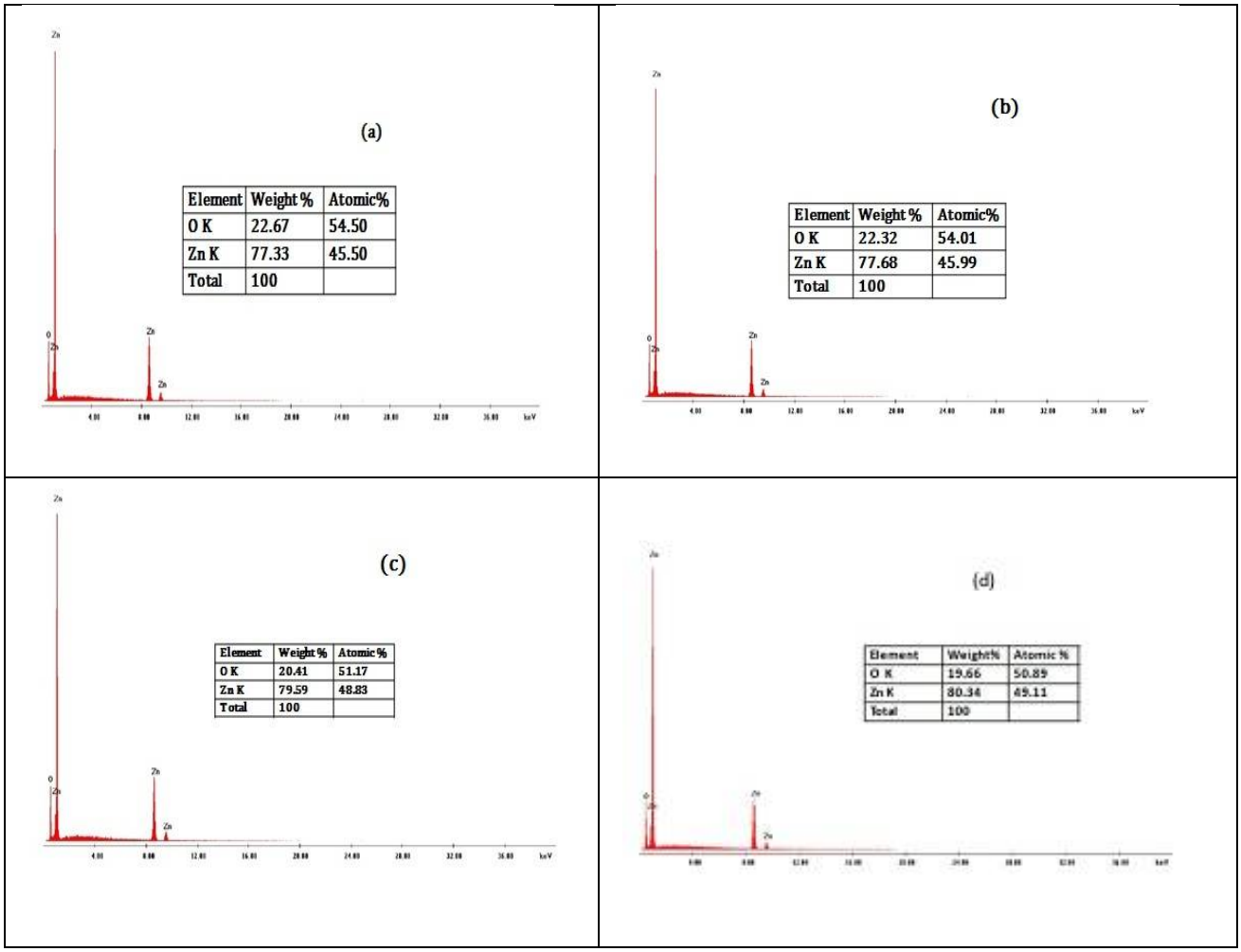

Fig.10 EDX spectra of ZnO thin films with molarities (a) 0.25M, (b) 0.50M ,(c) 0.75M and (d)1.00M

3.2 Scanning electron microscopy (SEM) and Energy dispersive X-rays (EDX) study

The surface morphology of the ZnO thin film deposited on the glass substrate at different precursor molarities which are observed in the SEM images shown in the Fig.9**.** The results showed that the thin films exhibit a uniform films are of good quality. The EDX spectrum and atomic composition of the ZnO/glass is shown in Fig.10. The EDX results show that there is no other impurity present in the films prepared. The morphology of the prepared films indicates that the particles are coated uniformly over the entire substrate. SEM results are found to be very good with nearly stoichiometric formation of ZnO nanocrystals of granular shape and obviously demonstrate aggregation of the particles in some places. In the sample of 0.25M some porosity is seen on the film but for other three films of molarity 0.50, 0.75 and 1.00 there is closely packed homogeneous nanostructure with absence of porosity.

3.3 Ultra High Resolution Transmission electron microscopy (UHRTEM)

The UHRTEM micrograph of ZnO sample of 0.25, 0.50 and 0.75 molarity is shown in Fig11. The image of ZnO samples show the granular shape and as molarity increases there shows aggregation of the particles. The aggregation of particles should had been originated from the large and specific surface area and high surface energy of ZnO

ISSN(Online) : 2319-8753
ISSN (Print) : 2347-6710

International Journal of Innovative Research in Science, Engineering and Technology

(An ISO 3297: 2007 Certified Organization)

Website: www.ijirset.com

Vol. 6, Issue 6, June 2017

nanoparticles [41].The aggregation occurred probably during the process of drying [42,43]. From TEM image the average particle size of the ZnO samples are found to be 36 nm, 39nm and 44 nm respectively which is very nearly

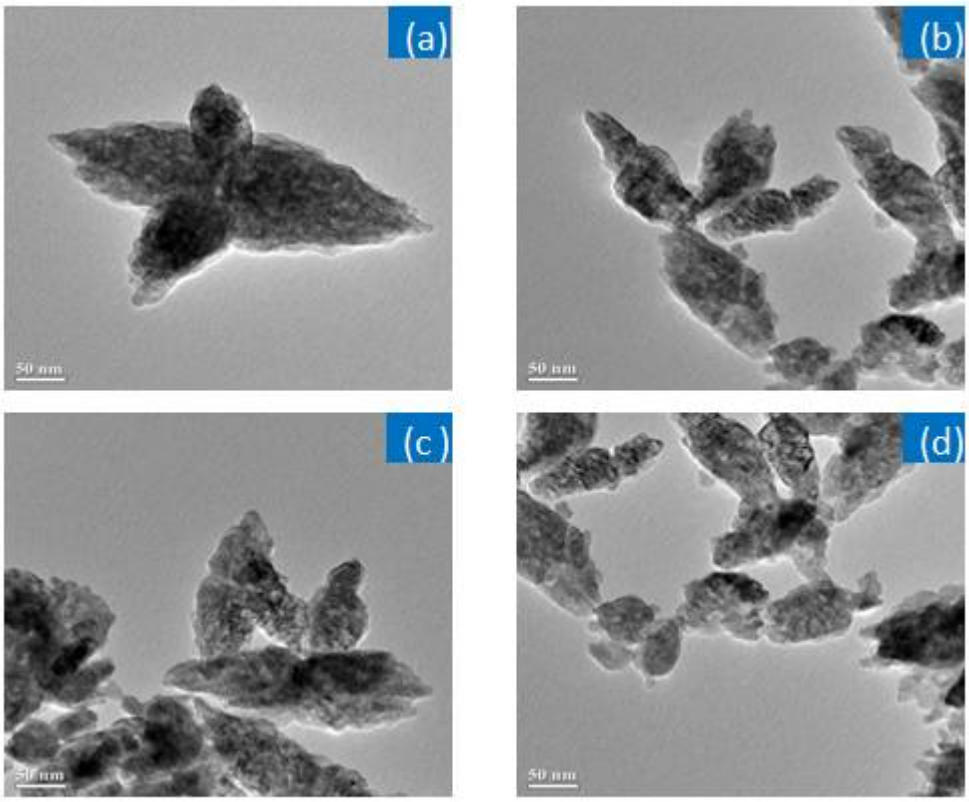

Fig. 11 UHRTEM micrograph of ZnO sample with (a) 0.25M, (b) 0.50 M (c) 0.75M and (d)1.00M

close to the result obtained based on XRD study by SSP method. The well crystallinity can be observed in lattice planes along (002) having values of d (interplanar spacing of the crystal planes) as 0.260nm [Fig. 12(a)] and Fig.12(b) shows selected area electron diffraction (SAED) pattern of the sample consisting of a central halo and concentric rings, which indicate the crystalline structure of the sample.

3.4 Optical properties

3.4.1UV-Vis Study

Fig.12 (A) shows the absorption spectrum of ZnO films coated on glass substrate. The absorption edge at 353 nm ,357 nm ,360 nm and 361nm are observed in the absorption spectrum for four samples of 0.25,0.50 , 0.75 and 1.00 molarity samples respectively. When the energy of a photon is equal to or greater than the band gap of the material, the photon is absorbed by the material and excites an electron into the conduction band where there occurs an abrupt increase in

ISSN(Online) : 2319-8753
ISSN (Print) : 2347-6710

International Journal of Innovative Research in Science, Engineering and Technology

(An ISO 3297: 2007 Certified Organization)

Website: www.ijirset.com

Vol. 6, Issue 6, June 2017

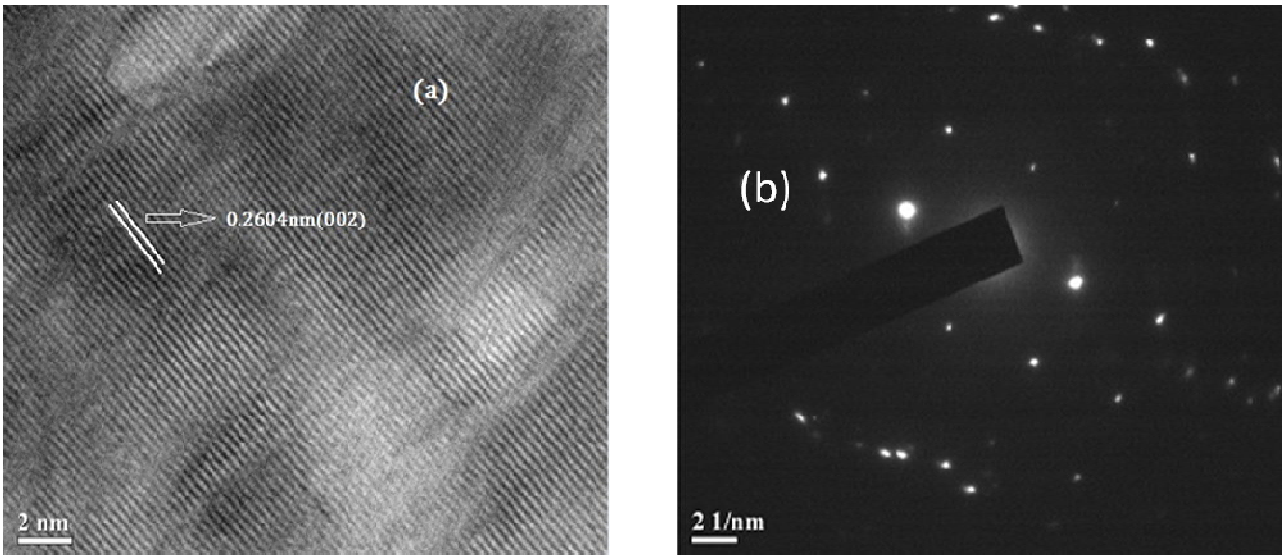

Fig. 12 (a) lattice planes and (b) SAED pattern of ZnO nanocrystals of molarity 0.25M .

the absorbency of the material to the wavelength corresponding to the band gap energy. The optical band gap E_g of the thin film was calculated from Tauc plot as shown in Fig.12 (B). The presences of single slope in the plot suggest that the film have direct and allowed transition. For such transition we have

$$(\alpha h\nu)^2 = A(h\nu - E_g)^n \quad (20)$$

where α is absorption coefficient, $h\nu$ is the incident photon energy, E_g represents the optical band gap, n is 1 for direct transition and A is constant. The band gap energy is obtained by extrapolating the linear portions of the plot to zero absorption coefficient. The band gap value of ZnO thin films are found to be 3.47 eV, 3.45eV , 3.38ev and 3.4 eV respectively for the films of molarities 0.25, 0.50 , 0.75 and 1.00 .These values show blue shift of band gap from its bulk value 3.37 eV due to weak quantum effect of prepared ZnO nanocrystals. The blue shift in the excitation absorption clearly indicates the quantum confinement property of nanoparticles. In the quantum confinement range, the band gap of the particles increases resulting in the shift of absorption edge to lower wavelength, as the particle size decreases. The decrease in the band gap when crystallite size increases has been reported in literature [44].

3.4.2Photoluminescence study

Photoluminiscence emission spectra were recorded by using F-2500 Fluroscence spectrophotometer in the wavelength range 325-800 nm with excitation wavelength of 325nm. The room temperature PL spectra of prepared nanocrystals are shown in Fig.12.Peaks were observed around 380nm (UV),475 nm (blue)and 555nm(green).The UV emission corresponds to the near band edge emission which is caused by annihilation of excitons by recombination[45-47]. The blue and green emissions results from the radiative recombinations of photo generated holes with singularly ionized oxygen vacancies[46] and oxygen related vacancies[47] respectively. The sharp intense UV emission indicates that ZnO nanocrystalline thin films are highly crystalline with excellent optical properties. As molaritiy of the precursor samples increases the intensities of emissions increases which may be due to decrease in the quantum size effect, surface area, and oxygen vacancy concentration, which are essential for intense emission [48].

ISSN(Online) : 2319-8753
ISSN (Print) : 2347-6710

International Journal of Innovative Research in Science, Engineering and Technology

(An ISO 3297: 2007 Certified Organization)

Website: www.ijirset.com

Vol. 6, Issue 6, June 2017

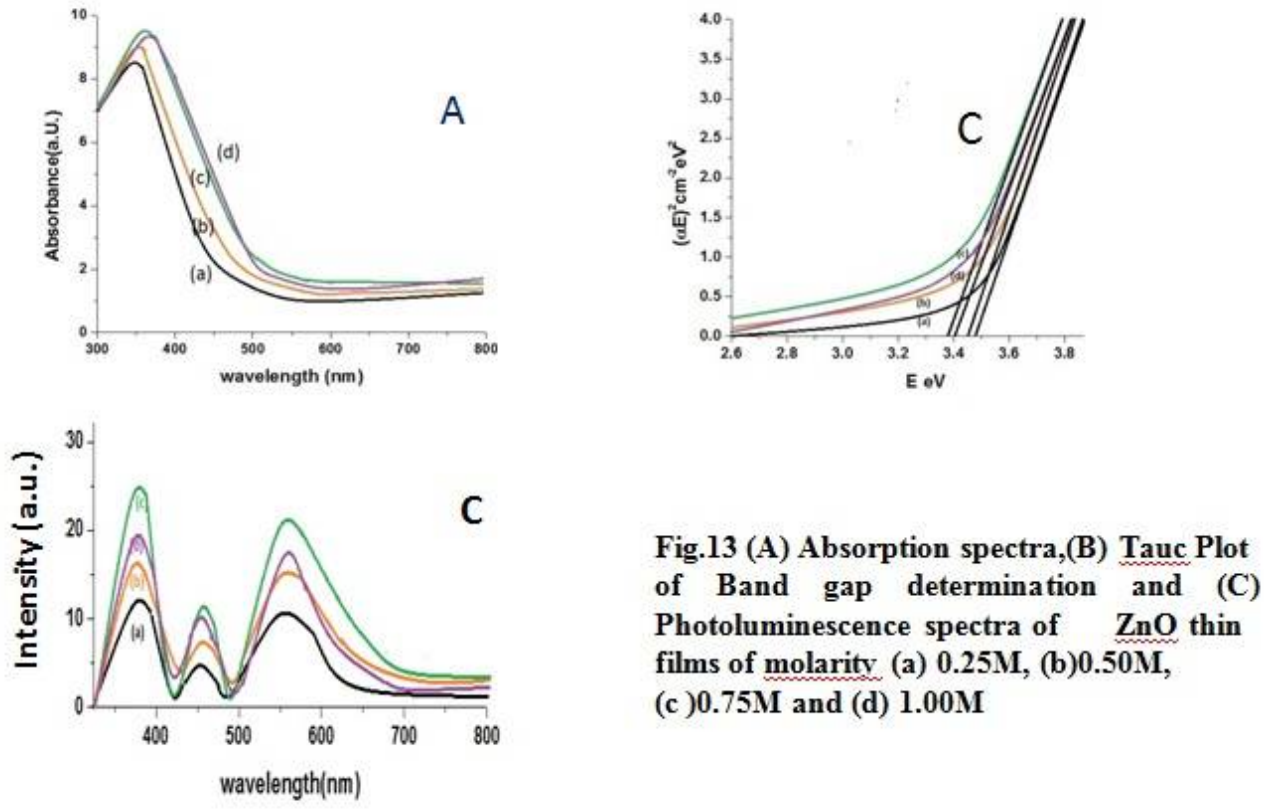

Fig.13 (A) Absorption spectra,(B) Tauc Plot of Band gap determination and (C) Photoluminescence spectra of ZnO thin films of molarity (a) 0.25M, (b)0.50M, (c)0.75M and (d) 1.00M

IV. CONCLUSION

Nanostructured ZnO films deposited by SILAR method are found to be uniform and have good adherence to the substrates. The formation of ZnO nanoparticles have been confirmed by XRD and UHRTEM analyses. The peak broadening was analyzed by the Scherrer's equation, SSP and W–H methods Some variation in the average crystallite size obtained from Scherrer's formula and W–H analysis is due to the difference in averaging the particle size distribution. From different methods it is seen that with the increase in molar concentration of the precursor solutions crystallite size of the prepared ZnO films increases upto some concentration of Zinc .Moreover, strain decreases as particle size increases. As the molarity increases optical absorbance edge shifted towards higher wavelength sides and red shift of optical band gap occurs. The photoluminescence of the ZnO composite nanostructures showed major bands in the UV, blue and green regions.

ACKNOWLEDGEMENTS

Authors would like to thank SAIF, Gauhati University, Guwahati ,India for XRD analysis and are also thankful to SAIF, NEHU , Shillong, India for TEM analysis. For optical characterization authors would like to thank Chemistry department of Gauhati university, Guwahati,India.

ISSN(Online) : 2319-8753
ISSN (Print) : 2347-6710

International Journal of Innovative Research in Science, Engineering and Technology

(An ISO 3297: 2007 Certified Organization)

Website: www.ijirset.com

Vol. 6, Issue 6, June 2017

REFERENCES

[1] V.S. Muralidharan, and A. Subramania, Nanoscience and technology, Crc Press, New Delhi, 2008, ISBN 9781420089622.
[2] B. C. Ejelonu, P. A. Ajibade, "ZnS, CdS and HgS "Nanoparticles in Poly(Methyl Methacrylate) Matrix :Synthesis,Thermal and Structural Studies",Chalcogenide Letters, vol.13,No 12,2016,pp 563-574.
[3] XL Xu ,SP Lau ,JS Chen ,GY Chen ,BK Tay, "Polycrystalline ZnO thin films on Si (100) deposited by filtered cathodic vacuum arc", J Cryst Growth vol.223,2001, pp 201–205.
[4] YC Liu ,SK Tung ,JH Hsieh , "Influence of annealing on optical properties and surface structure of ZnO thin films", J Cryst Growth ,vol.287,issue 1,2006, pp 105–111.
[5] T. Negami, Y. Hashimoto and S. Nishiwaki, "Cu(In,Ga)Se2 thin-film solar cells with an efficiency of 18%", Solar Energy Materials & Solar Cells, vol.67, 2001, p231.
[6] YF Lu ,HQ Ni ,ZH Mai,ZM Ren, "The effects of thermal annealing on ZnO thin films grown by pulsed laser deposition", J Appl Phys.,vol.88, 2000, p498.
[7] FK Shan ,GX Liu ,WJ Lee ,GH Lee , IS Kim ,BC Shin ,YC Kim , "Transparent conductive ZnO thin films on glass substrates deposited by pulsed laser deposition", J Cryst Growth,Vol. 277,2005, pp 284–292.
[8] Clement Yuen, SF Yu , SP Lau , CK Chen George , "Design and fabrication of ZnO light-emitting devices using filtered cathodic vacuum arc technique", J Cryst Growth ,vol. 287,2006, pp 204–212.
[9] XT Zhang , YC Liu ,ZZ Zhi , JY Zhang ,YM Lu , DZ Shen ,W Xu , GZ Zhong ,XW Fan , XG Kong , "Resonant Raman scattering and photoluminescence from highquality nanocrystalline ZnO thin films prepared by thermal oxidation of ZnS thin films", J Phys D Appl Phys., vol.34, 2001, p 3430.
[10] C Bundesmann , N Ashkenov, M Schubert ,D Spemann ,T Butz , EM Kaidashev , M Lorenz , M Grundmann, "Raman scattering in ZnO thin films doped with Fe, Sb, Al, Ga, and Li.", Appl Phys Lett., vol.83,2003, pp1974.
[11] S Amirhaghi , V Craciun , D Craciun , J Elders , IW Boyd, "Low temperature growth of highly transparent c-axis oriented ZnO thin films by pulsed laser deposition", Microelectron Eng, vol.25,1994, pp321–326.
[12] Park Tae Eun, Kim Dong Chan, Kong Bo Hyun, Cho Hyung Koun, "Structural and optical properties of ZnO thin films grown by rf magnetron sputtering on Si substrates", J Korean Phys Soc , vol.45,2004, pp 697–700.
[13] N Lehraki ,MS Aida ,S Abed , N Attaf , A Attaf , M Poulain , "ZnO thin films deposition by spray pyrolysis: influence of precursor solution properties", Curr Appl Phys., vol.12, 2012,pp1283–1287.
[14] A Zaier , El az F Oum, F Lakfif , A Kabir ,S Boudjadar , M S Aida, "Effects of the substrate temperature and solution molarity on the structural opto-electric properties of ZnO thin films deposited by spray pyrolysis", Mater Sci Semicond Process , vol.12, 2009, pp207–211.
[15] Jiwei Zhai, Liangying Zhang, Xi Yao. The dielectric properties and optical propagation loss of c-axis oriented ZnO thin films deposited by sol–gel process. Ceram Int., vol. 26,issue 8, 2000; pp883–885.
[16] K. V. Gurav, V. J. Fulari, U. M Patil, C. D. Lokhande and O. Joo, "Room temperature soft chemical route for nanofibrous wurtzite ZnO thin film synthesis", Appl. Surf. Sci., vol.256, 2010, pp2680-2685.
[17] F. Yakuphanoglu, Y. Caglar, S. Ilican and M. Caglar, "The effects of fluorin on the structural, surface morphologyand optical properties of ZnO thin films", Physica, B, vol. 394, No 86 ,2007.
[18] M. Ristov, G. J. Sinadinovski, I. Grozdanov and M. Mitreski, "Chemical deposition of ZnO films", Thin Solid Films, vol.149,No 65 ,1987.
[19] M. C. Sneed and R. C. Brasted, Comprehensive Inorganic Chemistry, Vol. 4, Princeton, New York, 1955.
[20] C E Rice, G S Tompa, L G Provost, N Sbrockey and J D Cuchiaro,"MOCVD Zinc Oxide Films For Wide Bandgap Applications," Mat. Res. Symp. Proc,Vol. 764,2003, p. 117.
[21] T. Mahalingam, , V.S. John, , M. Raja, , Y.K. Su, , P.J. Sebastian, "Electrodeposition and characterization of transparent ZnO thin films" Solar Energy Materials and Solar Cells, Volume 88, Issue 2, 2005, pp 227-235
[22] B. Cao, W. Cal, From ZnO nanorods to nanoplates: chemical bath deposition growth and surface-related emissions, J. Phys. Chem. C,vol.112, 2008,pp 680-685.
[23] D.D.O. Eya, A.J. Ekpunob, C.E. Okeke, Influence of thermal annealing on the optical properties of tin oxide thin films prepared by chemical bath deposition technique, Acad. Open Internet J. ,vol. 17 ,2006.
[24] S. Mondal and P. Mitra, "Effect of Manganese Incorporation in ZnO Thin Films Prepared by SILAR", Sci. & Soc., 10, No 2,2012.
[25] A. Ivanauskas, R. Ivanauskas, I. Ancutiene, "The Deposition of CuInSe2 Layer on glass substrate by SILAR Method", Chalcogenide Letters ,Vol. 13,No 8 ,2016, pp 373-380.
[26] N.Choudhury and B.K. Sarma, "Structural characterization of lead sulfide thin films by means of X-ray line profile analysis", Bulletin of Material Science, vol.32,No 1,2009,pp 43-47.
[27] V D Mote, Y Purushotham and B N Dole, "Williamson-Hall analysis in estimation of lattice strain in nanometer-sized ZnO particles",Journal of Theoretical and Applied Physics ,vol.6,No 6, 2012.
[28] P.K. Mochahari, Ananta Rajbongshi, Nava Choudhury, F. Singh, K.C. Sarma, "Study of chemically synthesized SHI irradiated CdS nanostructured films",Adv. Mater.Lett, vol. 6,No4,2015,pp 354-358.
[29] P K Mochahari and K C Sarma, "Study of structural and optical properties of chemically synthesized nanostructured cadmium zinc sulphide films for band gap tenability",Indian J Phys ,vol.90, No 1,2016,pp.21-27.
[30] Berestok T.O., Kurbatov D.I., Opanasyuk N.M, Pogrebnjak A.D., Manzhos O.P., Danilchenko S.M., "Structural Properties of ZnO Thin Films Obtained by Chemical Bath Deposition Technique", Journal of Nano- And Electronic Physics Vol. 5 ,No 1, 2013 ,pp01009-01013
[31] J B Nelson ,D P Riley , Proc. Phys. Soc. (London) 1945, 57, 160.
[32] Eman M. Nasir, International Review of Physics (I.Re.Phy.), Vol. 7, No 1, 2013.

ISSN(Online) : 2319-8753
ISSN (Print) : 2347-6710

International Journal of Innovative Research in Science, Engineering and Technology

(An ISO 3297: 2007 Certified Organization)

Website: www.ijirset.com

Vol. 6, Issue 6, June 2017

[33] S Sen, S K Halder and S P Sengupta, "An X-Ray Line Broadening Analysis in the Vacuum-Evaporated Silver Films", J. Phys. Soc. Jpn. ,vol.38, No 6 ,1975,pp1641-1647.
[34] Z.Yamlahi Alami, M. Salem, M. Gaidi,J.Elkhamkhami, "effect of Zn concentration on structural and optical proprieties of ZnO thin films deposited by spray pyrolysis", Advanced Energy: An International Journal (AEIJ), Vol. 2, No. 4, 2015,pp11-24
[35] A K Zak and W H A Majid, "Characterization And X-Ray Peak Broadening Analysis In PZT Nanoparticles Prepared By Modified Sol–Gel Method",Ceramic International ,vol.36,No 6,2010,pp 1905-1910.
[36] M A Tagliente and M Massaro, "Strain-driven (0 0 2) preferred orientation of ZnO nanoparticles in ion-implanted silica", Nuclear Instruments and Methods in Physics Research B, vol.266,2008,pp 1055–1061.
[37] P Rageswari and S Dhanuskodi, "Microstructural Effects of Mn2+ ions in ZnO Nanoparticles", Cryst. Res.Technol., vol.48,No 9 ,2013,pp 589-598.
[38] J. Zhang, Y. Zhang, K.W. Xu, V. Ji, "General compliance transfor- mation relation and applications for anisotropic hexagonal metals", Solid State Commun. Vol.139,2006,pp 87–91.
[39] J.F. Nye, Physical Properties of Crystals: Their Representation by Tensors and Matrices. Oxford, New York, 1985.
[40] A.K. Zak, M.E. Abrishami, W.H. Abd. Majid, R. Yousefi, "X-ray analysis of ZnO nanoparticles by Williamsone Hall and size strain plot Methods", Solid State Sciences ,vol.13,2011,pp 251-256
[41] Davood Raoufi, "Synthesis and photoluminescence characterization of ZnO nanoparticles", Journal of luminescence, vol.134,2013,pp 213-219.
[42] R.Y. Hong, J.Z. Qian, J.X. Cao, "Synthesis and characterization of PMMA grafted ZnO nanoparticles",Powder Technol.,vol.163,No3,2006,pp 160-168.
[43] R.Y. Hong, J.H. Li, L.L. Chen, D.Q. Liu,H.Z. Li, Y. Zheng, J. Ding, "Synthesis, surface modification and photocatalytic property of ZnO nanoparticles",Powder Technol.,vol.189,2008,pp 426-432
[44] P. Sagar ,P K Shishodia ,R.M. Mehra ,H Okada ,A Wakahara ,A Yoshida ,"Photoluminescence and absorption in sol–gel-derived ZnO films". J Lumin.,vol.126,No2,2007,pp800–806
[45] J.P.Kar,M.H.Ham,S.W.Lee,J.M.Myoung,"Fabrication of ZnO nanostructures of various dimensions using patterned substrates",Appl.Surf.Sci.,vol.255,2009,pp 4087–4092.
[46] L.Z.Pei,H.S.Zhao,W.Tan,H.Y.Yu,Y.W.Chen,W.F.Zhang,"Single crystalline ZnO nanorodsgrown by a simple hydrothermal process",Mater.Charact.,vol 60,2009, pp1063-1067.
[47] M.Qiu,Z.Ye,J.Lu,H.He,J.Huang,L.Zhu,B.Zhao,"Growth and properties of ZnO nanorods and nanonails by thermal evaporation",Appl.Surf.Sci., vol.255,2009,pp 3972–3976.
[48] Y. Masuda, M. Yamagishi, W. S. Seo, K. Koumoto, "Photoluminescence from ZnO nanoparticles Embedded in an Amorphous matrix",Cryst. Growth Des.,vol.8,No5, 2008, pp1503-1508.